Fractal Structure of TiH_2 Aggregates in a CuTi Matrix

Ph. Mangin[(a)]
Institut Laue-Langevin, F-38042 Grenoble Cédex, France

and

B. Rodmacq and A. Chamberod
Service de la Physique, Commissariat à l'Energie Atomique, Group de Metallurgie Physique, Departement de Recherche Fondamentale, Centre d'Etudes Nucléaires de Grenoble, F-38041 Grenoble Cédex, France

(Received 6 May 1985)

The evolution of TiH_2 aggregates formed from an amorphous hydrogenated CuTi alloy has been measured by small-angle neutron scattering as a function of temperature. The total correlation function has been used to determine both fractal dimension D and crossover length ξ which are found to increase with temperature. The temperature range studied can be divided into three regions corresponding respectively to the formation, restructuring, and growth of the aggregates. This evolution is related to the variation of the hydrogen content and to its mobility inside the sample.

PACS numbers: 61.40.Df, 05.40.+j, 61.12.Dw, 81.30.Mh

Studies of the aggregation of small particles to form clusters have been stimulated by a large variety of problems, such as branched polymers,[1,2] colloid aggregates,[3,4] coagulation of smoke particles,[5] and electrodeposited or sputter-deposited films.[6,7] Several aggregation models have been built up by computer simulation, such as the diffusion-limited aggregation model[8] or the kinetic clustering of clusters model.[9,10] In this latter case, the introduction of a sticking probability[11] allows chemical effects (e.g., restructuring during the growth) to be taken into account. These models lead to ramified structures with a fractal dimensionality D smaller than the corresponding Euclidean dimensionality d. A crossover from a fractal structure on a short length scale to a structure with uniform density on a long length scale has also been pointed out.[9,10]

In this Letter we present the clustering of TiH_2 in an amorphous CuTi matrix as an example of fractal precipitates. At high temperature, hydrogen desorption leads first to the increase of the fractal dimension from $D=2.1$ to $D=3$ without any change of the crossover length. Further hydrogen desorption corresponds to a progressive increase of this crossover length.

This study has been carried out by small-angle and large-angle neutron scattering at Institut Laue-Langevin (ILL) in Grenoble. This technique is particularly well adapted to our case because (i) one can study bulk samples, (ii) the combination of positive (copper) and negative (titanium and hydrogen) neutron scattering lengths results in a very good contrast between the TiH_2 precipitates and the CuTi matrix, and (iii) the large incoherent scattering cross section of hydrogen can be used to follow the variation of the hydrogen content of the sample.

For an infinite aggregate with fractal dimension D in a Euclidean space of dimension d, the correlation function is given by

$$C(r) = \langle \rho_\infty(0)\rho_\infty(r)\rangle \sim r^{-\alpha}, \tag{1}$$

in which $\alpha = d - D$. $\rho_\infty(u)$ is the density of particles in this *infinite* aggregate. This correlation function is only valid for $r >> a$, where a is a lower limit given by the size of the structural unit.

In a real system, the scale invariance is limited by a crossover length ξ. The true correlation function $g(r) \sim \langle \rho(0)\rho(r)\rangle$ is identical to $C(r)$ for $r << \xi$ and tends towards the mean density ρ_0 for larger distances. The kinetic clustering of clusters model[9,10] is a good example of this situation. Let us start with a uniform density of particles ρ_0; these particles then gather in "filled" areas of larger density with $C(r) \sim r^{-\alpha}$ and leave the remaining space "empty." The succession of such filled and empty areas maintains the average density ρ_0. The fractal law $C(r) \sim r^{-\alpha}$ is thus restricted to areas with a mean size ξ (see, for example, Fig. 1 of Meakin[9]). In order to take this limitation into account, Sinha, Freltoft, and Kjems[12] proposed that the correlation function $g(r)$ is of the form $g(r) \sim r^{-(d-D)} e^{-r/\xi}$. In their study of ultrafine smoke particles, Forrest and Witten[5] also showed that a better fit to the experimental data was obtained with such a correlation function.

We would like first to give a justification for such a correlation function. For length scales larger than ξ, the system can be viewed as a two-phase system with "filled" and "empty" areas. If the filled areas had a uniform density, the system would be described by the density function $\sigma(u)$ with $\sigma(u)=1$ in filled areas and $\sigma(u)=0$ in empty areas, and could be quite analogous to a porous material. In this case, and for a random distribution of empty areas (i.e., holes in a porous material), the correlation function in the

Debye-Bueche formalism[13,14] is given by

$$\gamma(r) \sim \langle \sigma(0)\sigma(r) \rangle \sim e^{-r/\xi}. \tag{2}$$

For short length scales, one has now to consider the fine structure of the filled areas with the corresponding correlation function $C(r)$ of Eq. (1). The theory of diffraction by a finite object can be used to determine the total correlation function $g(r)$.[15] Let us consider the filled areas as the object. $\rho_\infty(u)$ is the density of particles in an infinite object, $\sigma(u)$ is the form factor of the object; $\rho(u)$, the density of matter inside the object, can be written $\rho(u) = \sigma(u)\rho_\infty(u)$, with the corresponding correlation function

$$g(r) = \langle \sigma(0)\rho_\infty(0)\sigma(r)\rho_\infty(r) \rangle. \tag{3}$$

If there is no correlation between the shapes of the filled areas and the finite structure inside these areas, Eqs. (1)-(3) lead to

$$g(r) = \langle \rho_\infty(0)\rho_\infty(r) \rangle \langle \sigma(0)\sigma(r) \rangle \sim r^{-(d-D)} e^{-r/\xi}. \tag{4}$$

If the mean size of the filled areas and their fine structure are correlated, Eq. (4) is still valid provided that the shapes of the filled and empty regions are *randomly distributed* (this is the major assumption of Debye, Anderson, and Brumberger[14]).

The great interest of the correlation function of Eq. (4) is that it takes into account *both* the finite size and the fractal structure of the aggregates. It is clearly apparent from both computer simulations[8-10] and experiments on real systems[3,5-7] that, as a result of these finite-size effects, Eq. (1) cannot be used to reproduce the behavior of the correlation function on the whole range of r.

The corresponding diffracted intensity is given by a Fourier transform of Eq. (4). For $d=3$ one obtains

$$I(q) \sim \frac{\Gamma(D-1)\xi^D}{(1+q^2\xi^2)^{D/2}} \frac{(1+q^2\xi^2)^{1/2}}{q\xi} \times \sin[(D-1)\arctan(q\xi)] \tag{5}$$

with two particular cases: $D=3$, $g(r) \sim e^{-r/\xi}$, which gives the Debye law,

$$I(q) \sim \frac{\xi^3}{(1+q^2\xi^2)^2},$$

and $D=2$, $g(r) \sim r^{-1}e^{-r/\xi}$, which gives the Ornstein-Zernike law,

$$I(q) \sim \frac{\xi^2}{1+q^2\xi^2}.$$

In the case $a \ll r \ll \xi$, the term $r^{-\alpha}$ is dominant. It is thus possible to determine a q range ($q\xi \gg 1$) in which the scattering law is approximately given by $I(q) \sim q^{-D}$. Such a scattering law has been used to interpret small-angle x-ray scattering results in terms of fractal aggregates.[4] When $q\xi$ is of order of 1 to 10, it is necessary to use the total scattering function of Eq. (5) [in the same way as Eq. (1) cannot be used for $r \simeq \xi$]. Moreover, Eq. (5) shows that in this $q\xi$ range the apparent slope of $\log I$ vs $\log q$ can be found larger than $-D$ for dimensions larger than 2, and tends towards -4 as D approaches the value of 3. For $D=3$ one is left with the classical Porod law which corresponds to the large-angle limit of the Debye law.

The results presented here concern TiH_2 precipitates in a CuTi matrix obtained from an amorphous $Cu_{50}Ti_{50}$ sample containing 15% hydrogen. Both large-angle ($0.17 < q < 3.34$ Å^{-1}) and small-angle ($0.8\times10^{-2} < q < 6.3\times10^{-2}$ Å^{-1}) measurements were performed in order to follow the thermal evolution of the material. The samples were heated from 300 to 800 K at a constant rate of 0.7 °C/min and diffraction spectra were recorded during the heating process with an accumulation time of 10 min.

From the large-angle scattering curves, corrected for the contribution of the sample holder, the thermal evolution can be summarized as follows. At room temperature, hydrogen atoms are randomly distributed in Ti_4 tetrahedral sites,[16] as is generally the case for early-transition-metal–late-transition-metal amorphous alloys. As the temperature increases, finely dispersed TiH_2-like aggregates are formed in the amorphous matrix. The corresponding maximum observed in the diffraction curve at $q \simeq 0.5$ Å^{-1} increases and shifts towards smaller q, indicating that the aggregates grow as the temperature increases. They become large enough to give observable diffraction peaks from about 450 K. Such an evolution implies both a diffusion of hydrogen atoms and a reorganization of titanium atoms, which can be explained by the more favorable enthalphy of formation of TiH_2 (−125 kJ/g-at.) as compared to that of CuTi (−25 kJ/g-at.).[17] At 600 K the amorphous matrix crystallizes to give γ-CuTi. Hydrogen begins to leave the sample from about 680 K, as indicated by the decrease of the intense background due to the incoherent scattering of hydrogen. This is also confirmed by a simultaneous decrease of the intensity of the TiH_2 diffraction peaks and an increase of the γ-CuTi ones.

The small-angle scattering results have been analyzed in the region from 645 to 800 K. The experimental curves were corrected by subtraction of the room-temperature curve. This procedure eliminates the parasitic scattering, the sample-holder scattering, and any undesirable contribution such as surface scattering.[18] It also eliminates the incoherent scattering of hydrogen, but tends to overestimate the total background at high temperature when hydrogen leaves the sample. However, this does not affect our results if one considers that, contrary to the large-angle case, this incoherent contribution is a minor part of the total background which itself represents only about 1% of the signal due to the TiH_2 precipitates.

In the temperature range studied, the small-angle intensity can be well fitted by Eq. (5) without having to introduce any additional form factor as Sinha, Freltoft, and Kjems[12] did in their work on silica-particle aggregates (note that there is a typing error in their corresponding Eq. 4.4). Figure 1 compares experimental and calculated curves at various temperatures. A good agreement is observed in the whole temperature range. Less satisfactory fits are obtained at high temperature for large scattering angles. This is a consequence of the rapid decrease of I vs q (more than three decades at 788 K) and of the smaller intensity in this temperature range. The corresponding uncertainties on D and ξ can be estimated to be about 3% and 5%, respectively. These uncertainties are smaller at lower temperature where smaller average slopes are observed.

Figure 2 presents the temperature variation of D and ξ as obtained from the previous fits, along with that of the incoherent scattering of hydrogen determined from the large-angle scattering experiments. One can notice that for such values of the crossover length, no approximate law ($q\xi >> 1$ or $q\xi << 1$) can be used to fit the whole diffraction curve. This shows that the values of ξ and D are always significant and justifies the use of Eq. (5). The temperature range can be divided into three regions. In region I ($T \lesssim 680$ K) the hydrogen content is constant. The fractal dimension increases slowly from about 1.9 at 645 K to 2.1 at 680 K. Such a change can be considered as significant compared with the estimated uncertainty in this temperature range. In the meantime the crossover length increases slightly to the value of 60 Å. In region II (680 K $\lesssim T \lesssim$ 740 K), hydrogen begins to leave the sample. The fractal dimension increases from 2.1 to 3, whereas the crossover length remains practically unchanged. In region III ($T \gtrsim 740$ K), most of the hydrogen leaves the sample. Although no upper limit of D ($D \leq d$) was imposed in the fitting procedure, a plateau is reached at $D = 3.0 \pm 0.1$ In this region the crossover length increases sharply up to 150 Å at 800 K.

A consistent interpretation of these results can be given with reference to the chemical aggregation model,[11] even if the mechanism of formation and growth of the small initial clusters is probably closer to that of the evaporation and condensation of atoms proposed for spinodal decomposition.[19] After the aggregation of small clusters at low temperature, region I would correspond to the end of the formation of the fractal aggregates. At the end of region I the fractal dimension is found to be very close to that obtained from the chemical aggregation model. In region II, the increase of the fractal dimension corresponds to a restructuring of the aggregates. There is no modification of the distribution of the "filled" and "empty" areas, and so the crossover length remains constant at 60 Å,

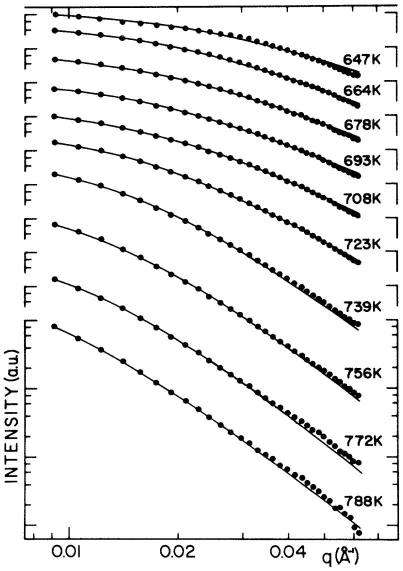

FIG. 1. Small-angle neutron scattering curves for TiH_2 aggregates at various temperatures and best fits by Eq. (5). The temperature increment between two successive curves is about 16 K. For clarity successive curves are shifted vertically by half a decade.

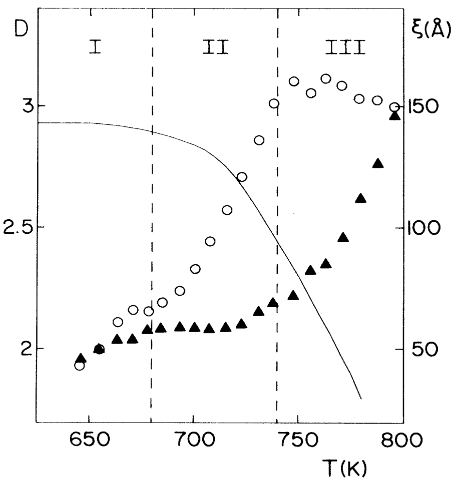

FIG. 2. Temperature variation of the fractal dimension (circles, left-hand scale) and crossover length (triangles, right-hand scale). The variation of the incoherent scattering of hydrogen (i.e., hydrogen content) is also shown (full line, arbitrary units).

but the TiH_2 aggregates are less and less ramified. The desorption of hydrogen observed in this region could correspond to the disappearance of the finest ramifications. In region III, the classical Debye law [$D = 3$ in Eq. (5)] accounts well for the variation of the scattering curves. The enhanced hydrogen mobility leads to a long-range reorganization of the structure as shown by the increase of the crossover length.

Such an evolution in regions II and III can well be compared to that obtained from Monte Carlo simulations by Heermann and Klein[20] on the nucleation and growth of spin droplets. These authors have observed a two-stage process in which a modification from a ramified structure to a more compact one at constant size is followed by classical growth with $D = 3$.

In conclusion, we have shown here an example of fractal structure obtained by a solid-state reaction. The use of a correlation function which takes into account both the fractal dimension and the finite size of the aggregates results in a very good agreement between experimental and calculated scattering curves in the whole temperature range. As followed by small-angle neutron scattering, the restructuring of TiH_2 aggregates is induced by hydrogen desorption and corresponds to a change in the fractal dimension of these aggregates. The role of the amorphism of the CuTi matrix in the formation of the fractal aggregates is not yet fully understood. Nevertheless the enhanced mobility of hydrogen in the amorphous CuTi hydrides[21] is certainly an important factor in this process.

We would like to thank L. Billard and M. Roth for helpful discussions and comments.

---

[a] Permanent address: Centre National de la Recherche Scientifique (CNRS), LA 155, Université de Nancy I, c.o. 140, F-54037 Nancy Cédex, France.

[1] H. J. Herrmann, D. P. Landau, and D. Stauffer, Phys. Rev. Lett. **49**, 412 (1982).

[2] D. W. Schaefer and K. D. Keefer, Phys. Rev. Lett. **53**, 1383 (1984).

[3] D. A. Weitz and M. Oliveira, Phys. Rev. Lett. **52**, 1433 (1984).

[4] D. W. Schaefer, J. E. Martin, P. Wiltzius, and D. S. Cannell, Phys. Rev. Lett. **52**, 2371 (1984).

[5] S. R. Forrest and T. A. Witten, Jr., J. Phys. A **12**, L109 (1979).

[6] M. Matsushita, M. Sano, Y. Hayakawa, H. Honjo, and Y. Sawada, Phys. Rev. Lett. **53**, 286 (1984).

[7] W. T. Elam, S. A. Wolf, J. Sprague, D. U. Gubser, D. Van Vechten, G. L. Barz, Jr., and P. Meakin, Phys. Rev. Lett. **54**, 701 (1985).

[8] T. A. Witten, Jr., and L. M. Sander, Phys. Rev. Lett. **47**, 1400 (1981).

[9] P. Meakin, Phys. Rev. Lett. **51**, 1119 (1983).

[10] M. Kolb, R. Botet, and R. Jullien, Phys. Rev. Lett. **51**, 1123 (1983).

[11] M. Kolb and R. Jullien, J. Phys. (Paris), Lett. **45**, L977 (1984).

[12] S. K. Sinha, T. Freltoft, and J. Kjems, in *Kinetics of Aggregation and Gelation,* edited by F. Family and D. P. Landau (North-Holland, Amsterdam, 1984), p. 87.

[13] P. Debye and A. M. Bueche, J. Appl. Phys. **20**, 518 (1949).

[14] P. Debye, H. R. Anderson, Jr., and H. Brumberger, J. Appl. Phys. **28**, 679 (1957).

[15] A. Guinier, *X-Ray Diffraction in Crystals, Imperfect Crystals, and Amorphous Bodies* (Freeman, San Francisco, 1963), Chap. 2.

[16] B. Rodmacq, Ph. Mangin, and A. Chamberod, J. Phys. F **15**, 2259 (1985).

[17] A. J. Maeland, in *Metal Hydrides,* edited by G. Bambakidis (Plenum, New York, 1981), p. 177.

[18] B. Rodmacq, Ph. Mangin, and A. Chamberod, Phys. Rev. B **30**, 6188 (1984).

[19] P. Mirold and K. Binder, Acta Metall. **25**, 1435 (1977).

[20] D. W. Heermann and W. Klein, Phys. Rev. Lett. **50**, 1062 (1983).

[21] R. C. Bowman, Jr., and A. J. Maeland, Phys. Rev. B **24**, 2328 (1981).